Analytica Chimica Acta xxx (2015) 1–8

Contents lists available at ScienceDirect

Analytica Chimica Acta

journal homepage: www.elsevier.com/locate/aca

Label-free detection of rheumatoid factor using YbY_xO_y electrolyte–insulator–semiconductor devices

Tung-Ming Pan [a, *], Ting-Wei Lin [b], Ching-Yi Chen [a]

[a] Department of Electronics Engineering, Chang Gung University, Taoyuan 33302, Taiwan
[b] School of Medicine, Chang Gung University, Taoyuan 33302, Taiwan

HIGHLIGHTS

- Effect of yttrium content on the structural and sensing properties of YbY_xO_y sensing membrane was explored.
- YbY_xO_y EIS device prepared at the 60 W condition exhibited good sensitivity characteristics.
- EDC–NHS functionalized of RF antibody and subsequently immobilized on the EIS shows a high sensitivity in the range 10^{-7}–10^{-3} M.

GRAPHICAL ABSTRACT

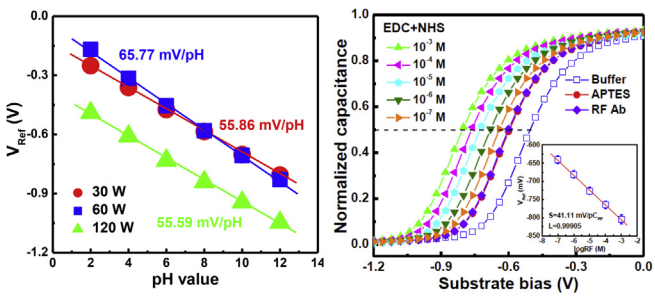

ARTICLE INFO

Article history:
Received 5 June 2015
Received in revised form
11 August 2015
Accepted 13 August 2015
Available online xxx

Keywords:
Biosensor
Electrolyte–insulator–semiconductor (EIS)
Immobilization
Rheumatoid factor (RF)
YbY_xO_y

ABSTRACT

In this study, we investigated the effect of yttrium content on the structural properties and sensing characteristics of YbY_xO_y sensing membranes for electrolyte–insulator–semiconductor (EIS) sensors to detect the rheumatoid factor (RF). The YbY_xO_y EIS device prepared at the 60 W plasma condition exhibited a higher sensitivity of 65.77 mV/pH, a lower hysteresis voltage of ~1 mV, and a smaller drift rate of 0.14 mV/h than did those prepared at the other conditions. We attribute this behavior to the optimal yttrium content in the YbY_xO_y film forming a smooth surface. Furthermore, we used a novel $YbTi_xO_y$ EIS biosensor to measure the RF antigen in human serum because of its rapid and label-free detection. Two different techniques were used for the immobilization of RF antibody onto the surface of an $YbTi_xO_y$ EIS sensor. The RF antibody was directly immobilized on the EIS surface modified with 3-aminopropyltriethoxysilane (APTES) followed by glutaraldehyde (GA). In contrast, a mixture of 1-ethyl-3-(3-dimethylamino-propyl)carbodiimide (EDC) and N-hydroxysuccinimide (NHS) solution was used to functionalize the carboxyl groups at the tail of RF antibodies. RF antibodies functionalized with the active NHS esters were covalently immobilized on the APTES-modified $YbTi_xO_y$ surface. The immobilized RF antibodies on the EIS that are functionalized with the EDC and NHS exhibit higher (41.11 mV/pC_{RF}) for detection of serum RF antigen in the range 10^{-7} to 10^{-3} M, compared to traditional antibody immobilization technique via APTES and GA linkage. The $YbTi_xO_y$ EIS biosensor is a promising analytical tool for RF antigen monitoring due to its good sensitivity, stability and repeatability.

1. Introduction

Rheumatoid arthritis (RA) is the most common autoimmune

* Corresponding author.
E-mail address: tmpan@mail.cgu.edu.tw (T.-M. Pan).

http://dx.doi.org/10.1016/j.aca.2015.08.014
0003-2670/

disease, affecting approximately 1% of the world's population [1]. Autoimmune disease is an illness that occurs when the body tissues are mistakenly attacked by its own immune system. Patients suffering from autoimmune diseases tend to have unusual antibodies circulating in their blood that target their own body tissues to cause systemic inflammation. The inflammation of the tissues around the joints and inflammatory arthritis are characteristic features of RA, but the disease can also cause inflammation and injury in other organs in the body. However, RA is generally a progressive disease that has the potential to cause persistent synovitis, pain, joint destruction, and functional disability. Rheumatoid factor (RF), i.e. immunoglobulins directed against the F_c region of IgG and IgM [2,3], has been employed as a diagnostic marker for RA in the current criteria. According to 2010 American College of Rheumatology/European League Against Rheumatism (ACR/EULAR) classification criteria for RA, the normal level of RF antigen in blood is below 2.59×10^{-6} M (40 IU/ml). RF can be measured using agglutination (e.g. latex agglutination test, LAT) [4], immunoassay (e.g. enzyme-linked immunosorbent assay, ELISA) [5] or quartz crystal microbalance (QCM) [6] method. However, none of these methods provides a user friendly procedure and high enough sensitivity at the same time. LAT provides a simple and rapid diagnostic method, but it has higher limit of detection and does not provide quantitative result. ELISA method is expensive and there occurs false positive or false negative result. In addition, the crystal surface of QCM sensor is not easily regenerated due to the analyte contamination of the quartz from previous measurements.

Ion-sensitive field-effect transistors (ISFETs) have been of great interest for highly sensitive and selective detection of biological and chemical species, because they can detect biomolecular interactions in a label-free manner through a direct change in conductance or a related electrical characteristic. An ISFET device is the modification of a metal-oxide-semiconductor field-effect transistors (MOSFET) where the gate electrode is replaced by an ion-selective membrane, an electrolyte solution and a reference electrode. At the interface of the gate oxide and electrolyte, the surface potential is generated by the process of ion or electron exchange. The interface can be modified by applying an ion-selective membrane to make the ISFET selective for specific target molecules [7]. Compared with an ISFET sensor, an electrolyte–insulator–semiconductor (EIS) device has a simpler fabrication process. Various gate oxide materials, such as SiO_2, Al_2O_3, Si_3N_4, Ta_2O_5 [8,9], have been employed as pH-sensing membranes due to their higher pH response. However, it is not easy to make a reliable sensing membrane in an ISFET device which has low pH sensitivity and stability [10,11]. Therefore, high-dielectric constant (high-κ) gate dielectric materials, including TiO_2, Y_2O_3, HfO_2, ZrO_2 [12,13], have been investigated as pH-sensitive membranes in ISFET or EIS devices. In recent years, tremendous research efforts have been focused on the investigation of rare-earth (RE) oxide films for the potential replacement of a conventional SiO_2 gate dielectric in advanced metal-oxide-semiconductor (CMOS) technologies [14,15]. The Yb_2O_3 thin film is a very promising candidate as a gate dielectric in CMOS devices because it has a high dielectric constant, wide band gap, and large conduction band offset with respect to silicon [15,16]. In our previous reports [17,18], we also showed that an Yb_2O_3 gate dielectric had a large capacitance value, low interface trap density, small hysteresis voltage as well as low frequency dispersion. However, the biggest issue during the use of RE oxide films is moisture absorption, which influences their sensing performance due to the formation of a hydroxide layer. The moisture absorption is attributed to the oxygen vacancies in the films [19]. To overcome this problem, the incorporation of other elements (Ti, or Y) into the RE dielectric films can suppress the moisture absorption of RE oxide film [20,21].

The surface modification can be used for the immobilization of biomolecules or recognition ligands to prevent nonspecific interaction or biomolecule adsorption. A direct surface modification approach based on silanization with 3-aminopropyltriethoxysilane (APTES) and activation with glutaraldehyde (GA) was developed by Williams and Blanch [22]. However, a direct immobilization method reduces the antigen-binding ability due to random orientation and/or denaturation [23–25]. Therefore, controlled and oriented immobilization of antibodies onto the sensor surface are required to promote the number of available antigen-binding sites and prevent the surface degradation. Dixit et al. [26] reported that 1-ethyl-3-(3-dimethylamino-propyl)carbodiimide (EDC) and N-hydroxysulfosuccinimide (SNHS) were used as heterobifunctional cross-linker molecules to immobilize antibodies on the aminated surface. This EDC/SNHS complex binds to the carboxyl-terminal of the antibodies, thus enhancing the combination an antigen with its antibody. The aim of this study was to develop an EIS-based biosensor for the detection of serum RF. Auger electron spectroscopy (AES) and atomic force microscopy (AFM) were used to explore the structural and morphological features of the YbY_xO_y sensing films and to provide the optimal Y content. We also examined the sensing characteristics (pH sensitivity, hysteresis, and drift) of the YbY_xO_y EIS sensor. Moreover, we compared two surface modification methods for RF antibody-immobilized EIS sensors. When the YbY_xO_y surface was treated with APTES, then the amine group of APTES reacted with GA to produce the aldehyde group. The RF antibody was directly immobilized on an aldehyde group-modified EIS surface. In contrast, a mixture of EDC and N-hydroxysuccinimide (NHS) in water was employed for activation of carboxyl groups at the tail of RF antibodies. The NHS ester-activated RF antibody was immobilized on an amine group-functionalized YbY_xO_y surface. Finally, we used two different surface-modified YbY_xO_y EIS biosensors to detect serum RF.

2. Materials and methods

2.1. Fabrication of YbY_xO_y EIS sensor

The EIS sensor structure featuring an YbY_xO_y sensing film was fabricated on 4-in p-type (100) Si wafer. Before the deposition of YbY_xO_y film, the wafers were cleaned using a standard Radio Corporation of America (RCA) process. A ~40 nm YbY_xO_y film was deposited on the Si substrate through co-sputtering from both ytterbium and yttrium targets in diluted O_2. The power conditions during co-sputtering were 100 W for Yb and 30, 60, and 120 W for Y. Then, the wafers were annealed by rapid thermal annealing (RTA) at 800 °C in O_2 ambient for 30 s. The thicknesses of YbY_xO_y films treated at the 30, 60, and 120 W plasma conditions were 39.2, 40.6, and 41.7 nm, respectively. An Al film (~300 nm) was then deposited on the backside of the Si wafer. Subsequently, an adhesive silicone gel (S181) was used to define the sensing area through a robotic dispensing system. Finally, EIS devices were fabricated on the copper lines of a printed circuit board with an Ag gel. An epoxy package was employed to encapsulate the EIS structure and the Cu line.

The compositional properties of the YbY_xO_y sensing films prepared under three Y plasma conditions were investigated using AES. In AES measurement, the Al K_α line at 1486.7 eV was used as the X-ray source, whereas the energy and current of the incident electron beam were set at 3 keV and 10 mA, respectively. The surface morphologies of the YbY_xO_y films were examined by AFM operated in the tapping mode; the scan size for the measurement of surface roughness was 3 μm.

Please cite this article in press as: T.-M. Pan, et al., Label-free detection of rheumatoid factor using YbY_xO_y electrolyte–insulator–semiconductor devices, Analytica Chimica Acta (2015), http://dx.doi.org/10.1016/j.aca.2015.08.014

2.2. pH sensing performance of YbY_xO_y EIS sensor

The pH sensitivity of the YbY_xO_y sensing films was determined by measuring the capacitance–voltage (C–V) curves of the EIS devices. The C–V curves for different pH buffer solutions (Merck Ltd., Taiwan) were measured using a Ag/AgCl reference electrode and a Hewlett–Packard (HP) 4284A LCR meter operated at an ac signal frequency of 500 Hz. To avoid light and noise interference, all the experimental setups were kept in the dark and performed at room temperature.

2.3. Surface modification of an YbY_xO_y EIS biosensor

In this paper, two modification methods were used to immobilize the RF antibody on the YbY_xO_y surface. One method was using APTES and GA to functionalize YbY_xO_y surface, which in turn yielded aldehyde groups on an EIS surface. The EIS device was immersed into the 2% APTES solution for 48 h to form a self-assembled monolayer on the YbY_xO_y membrane surface and then washed with deionized (DI) water. The functionalization of the EIS device was performed through APTES to convert metal hydroxide groups (M–OH) to amine (NH_2) groups on its surface. Next, the amine-functionalized YbY_xO_y surface was immersed in a 2.5% GA aqueous solution at 70 °C for 30 min, followed by rinsing with deionized water. Finally, the immobilization of RF antibody was achieved by exposing the aldehyde-functionalized YbY_xO_y surface to 10 μl RF antibody (1 mg/ml) in 10× phosphate-buffered saline (PBS) solution at 4 °C for 4 h, followed by washing of the unreacted surface aldehyde by PBS with 0.05% Tween 20 and subsequent drying in nitrogen ambient. The RF antibody and antigen were used human plasma (Biorbyt Ltd.). The other was using only APTES to treat the YbY_xO_y surface to produce amine groups on an EIS surface. 0.1 mmol EDC and 0.25 mmol NHS were dissolved in 5 ml of PBS at pH 6. RF antibody (10 μl) was treated with a 10 μl solution containing mixture of 20 mM EDC and 50 mM NHS for 15 min at 25 °C to activate the COOH-terminus of its antibody. Subsequently, the NHS ester-activated RF antibody solution was dripped on the EIS sensor with the NH_2-terminus of APTES for 2 h at 25 °C. Finally, EIS sensor was washed by PBS with 0.05% Tween 20 and subsequently dried in nitrogen ambient. RF antigen solutions with concentrations of 10^{-7}, 10^{-6}, 10^{-5}, 10^{-4}, and 10^{-3} M were prepared from RF antigen solution and PBS. For a given experiment, each condition was tested in triplicate.

3. Results and discussion

3.1. Structural properties of YbY_xO_y sensing films

In this study, we examined the composition and surface roughness of YbY_xO_y sensing films prepared under three Y plasma powers. Fig. 1 displays the AES depth profiles of Yb, Y, and O elements in the YbY_xO_y films under different Y power conditions. The film fabricated under three plasma powers showed a uniform composition profile through the film depth. The content of Y increases from ~1 to ~10 at.% with the increase in Y plasma power from 30 to 120 W. Under the 60 W condition, the Yb, Y and O concentrations versus thin film depth stayed constant in the bulk with an O content of roughly 50 at.% and a Yb:Y ratio of roughly 8:1, as shown in Fig. 1(b). In the AES profile, the O content in the film treated at the 30 W condition is almost the same as that at the 60 W condition, whereas the Yb:Y ratio decreases with increasing the Y plasma power. Furthermore, the Yb:Y ratio of the film prepared under the 120 W condition is approximately 3:1.

Fig. 2 shows the AFM images of the YbY_xO_y sensing films under three Y plasma powers. The YbY_xO_y film prepared at the 120 W condition exhibits the largest surface roughness (R_{rms} = 2.46 nm) among the plasma conditions. This result may be attributed to the high yttrium content in the film producing high density of chemical defects. Therefore, during high-temperature annealing, an increased self-diffusion of ytterbium and yttrium in the film results in the enhancement of the clustering of grains, thus increasing the surface roughness of the YbY_xO_y film. On the contrary, the YbY_xO_y sample prepared at the 60 W condition has a smooth surface (R_{rms} = 1.60 nm) due to the optimal yttrium content in the film. Furthermore, the sample treated at the 30 W shows a larger surface roughness of 2.11 nm than that at 60 W. The rougher surface may be attributed to the moisture absorption of YbY_xO_y because of less content of Y in the film to produce the oxygen vacancies, causing the nonuniform volume expansion of the film [23].

3.2. Performance of YbY_xO_y EIS pH sensors

Processes at the electrolyte/insulator interface of an ISFET (EIS) device are explained by the site-binding theory to describe the equilibrium between the amphoteric surface sites and the H^+ ions in the solution [27]. This theory takes into account the density of surface sites, surface complexation, and dissociation of surface sites, as well as electrical double layer (Gouy–Chapman–Stern model) [28]. The background electrolyte ions play a very important role in the formation of surface charge due to their specific interactions with surface hydroxyl groups (–OH) of metal oxide. The flatband voltage (V_{FB}) of an ISFET (or EIS) device is the most important measurable parameter; it is defined by the following equation [28]:

$$V_{FB} = E_{ref} - \Psi_0 + \chi^{sol} - \frac{\Phi_{Si}}{q} - \frac{Q_{ss} + Q_{ox}}{C_{ox}} \tag{1}$$

where E_{ref} is the reference electrode potential, ψ_0 is the surface potential, χ^{sol} is the surface dipole potential of the solution, Φ_{Si} is the silicon workfunction, q is the electron charge, Q_{ss} is the interface trapped charge, Q_{ox} is the fixed oxide charge, and C_{ox} is the gate insulator capacitance. All terms are constant except ψ_0, ψ_0 is the EIS sensitivity to the electrolyte pH that controls, which is controlling the dissociation of the oxide surface groups. The surface of metal oxide is rich in hydroxyl groups that can be found in a neutral state M–OH, a positive (protonated) state $M–OH^+_2$, or a negatively (deprotonated) state $M–O^-$ [28]. The transduction of pH to a potential difference ψ_0 between oxide surface and bulk solution is accomplished through a proton or hydroxide concentration. From the relation between gate oxide surface pH and bulk solution pH, the sensitivity of the surface potential to changes in the bulk pH can be obtained and is expressed in the following equation [29]:

$$\frac{\partial \Psi_0}{\partial pH} = -2.303 \frac{k_B T}{q} \alpha \tag{2}$$

$$\text{with} \quad \alpha = \frac{1}{1 + k_B T C_{DL} / q^2 \beta_{\text{int}}} \tag{3}$$

where α is the dimensionless sensitivity parameter. This value be related to the capacitance of the double layer (C_{DL}) and the intrinsic buffer capacity of the sensing layer surface (β_{int}). Based on equations (1) and (2), it can be concluded that the variation of pH causes the change in surface potential and thus affects the change in flatband voltage.

The effect of the Y content on the pH sensitivity of the YbY_xO_y sensing films can be understood by combining the site-binding and Gouy–Chapman–Stern interface to elucidate the ionic absorption processes at the electrolyte/membrane interface. To evaluate the

Please cite this article in press as: T.-M. Pan, et al., Label-free detection of rheumatoid factor using YbY_xO_y electrolyte–insulator–semiconductor devices, Analytica Chimica Acta (2015), http://dx.doi.org/10.1016/j.aca.2015.08.014

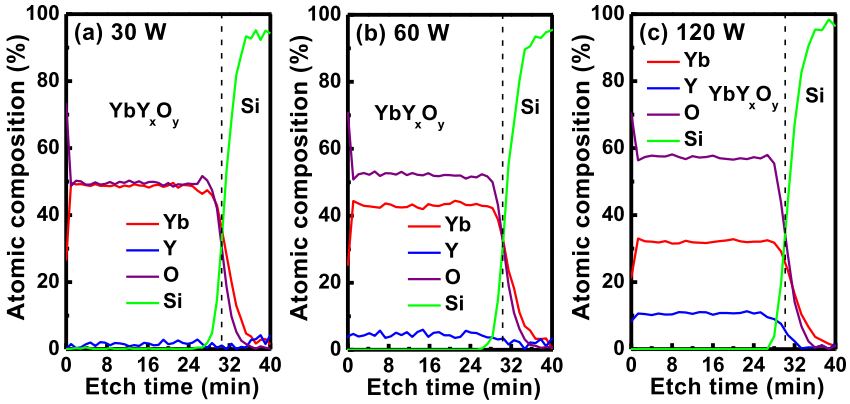

Fig. 1. Auger depth profiles of YbY_xO_y films fabricated at (a) 30 W, (b) 60 W and (c) 120 W conditions.

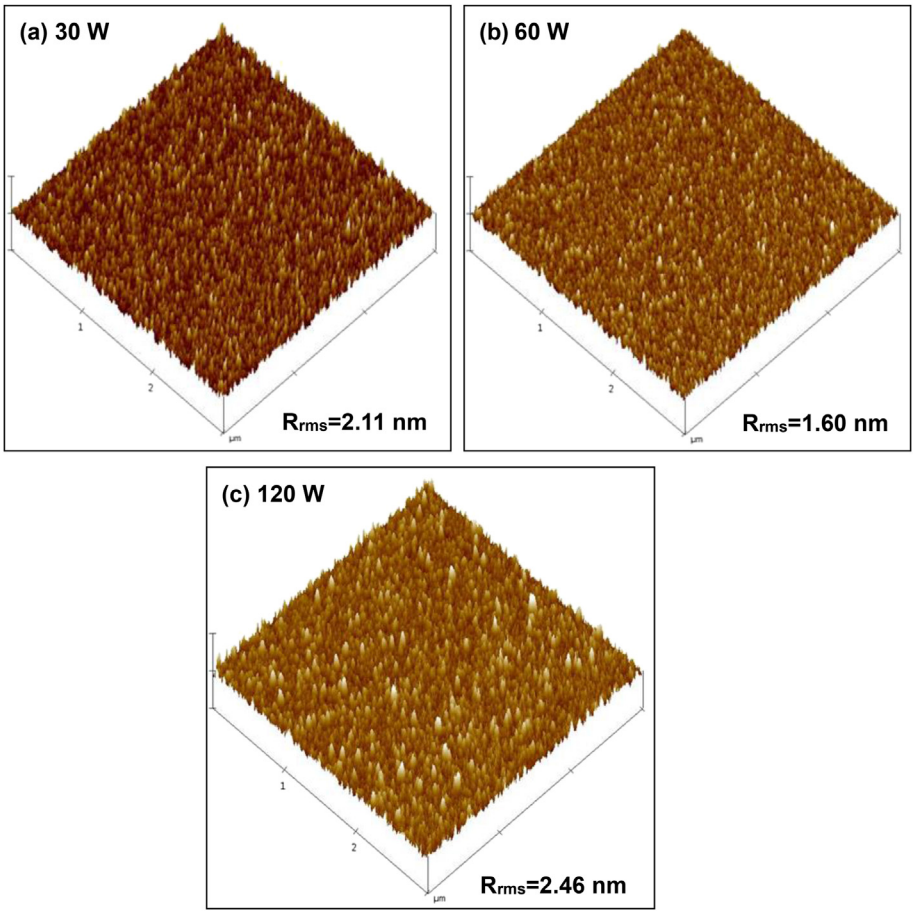

Fig. 2. AFM images of YbY_xO_y films fabricated at (a) 30 W, (b) 60 W and (c) 120 W conditions.

pH sensing performance of YbY_xO_y EIS sensors prepared under different Y plasma powers, we examined their behavior toward standard buffer solutions having pH values in the range 2–12. In EIS pH sensing, a change in pH normally causes a flatband voltage shift of the *C–V* curves, mainly due to the ionization of surface OH groups by H^+ or OH^- ions [30], in turn modifies the surface potential through dipole formation on the sensing membrane. Fig. 3(a)–(c) show the pH dependence of the normalized *C–V* curves for the YbY_xO_y EIS devices treated at the 30, 60, and 120 W plasma powers. Here, the reference voltage (V_{Ref}) was evaluated from the obtained *C–V* curves at a normalized capacitance of 0.5 [30]. To evaluate the sensing performance of an YbY_xO_y EIS device, we recorded a set of *C–V* curves at the pH ranging from 2 to 12. Fig. 3(d) depicts the pH dependence of the V_{Ref} of the YbY_xO_y EIS sensors prepared under three Y plasma conditions. During a cycle from pH 2 to 12, the YbY_xO_y EIS device prepared at the 60 W condition exhibits the highest pH sensitivity (65.77 ± 2.65 mV/pH) among these conditions (55.86 ± 3.12 mV/pH for 30 W and 55.59 ± 2.47 mV/pH for 120 W). This result could be attributed to the optimal yttrium content in the YbY_xO_y to reduce its oxygen

Please cite this article in press as: T.-M. Pan, et al., Label-free detection of rheumatoid factor using YbY_xO_y electrolyte–insulator–semiconductor devices, Analytica Chimica Acta (2015), http://dx.doi.org/10.1016/j.aca.2015.08.014

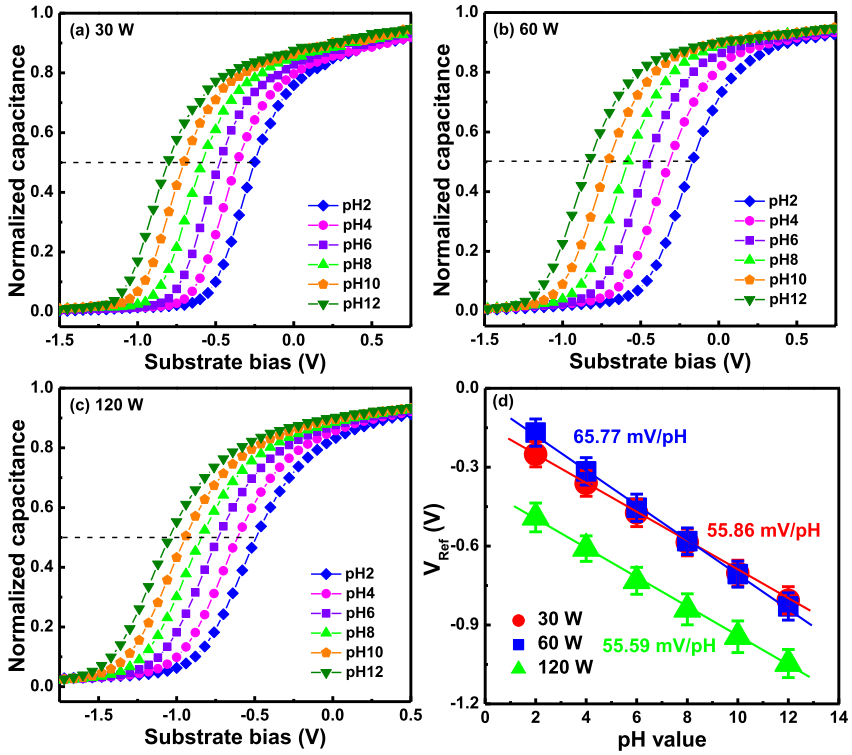

Fig. 3. A typical set of normalized *C*–*V* curves for the YbY_xO_y EIS sensor fabricated at (a) 30 W, (b) 60 W and (c) 120 W conditions in the concentration range from pH 2 to pH 12. (d) The calibration curve of the pH sensitive EIS sensors fabricated at different Y plasma powers. Error bars were calculated from the mean values, n = 3.

vacancy. The super-Nernstian pH response of an YbY_xO_y EIS sensor may be attributed to the high surface binding site density interacting with electrolyte ions, leading to increase in the compact-layer capacity to change in the number of transferred electron per unit of H^+ ion [31]. In this study, the EIS sensor featuring an YbY_xO_y sensing film demonstrated superior pH detection sensitivity than ISFET, extended gate field-effect transistor (EGFET), or EIS sensors using Al_2O_3 (54–56 mV/pH) [32], TiO_2 (58.21 mV/pH) [11], Ta_2O_5 (56–58 mV/pH) [32], ZrO_2 (55 mV/pH) [13], Y_2O_3 (54.5 mV/pH) [12], and ZnO_2 (58.13 mV/pH) [33] sensing films.

The long-term stability of a pH sensor device is hindered by the memory effects such as the hysteresis and drift [34]. Fig. 4(a) shows the hysteresis characteristics (reference voltage variation) of the YbY_xO_y sensing films prepared under different Y plasma powers during the pH loop of 7 → 4 → 7 → 10 → 7 over a period of 1500 s. Hysteresis effect can occur due to defects in a sensing film, giving rise to the formation of porous structures [10]. The interior sites of these porous defects can react with ions present in the solution, hence resulting in a hysteresis response. The YbY_xO_y EIS sensor prepared at the 60 W condition exhibits a lower hysteresis voltage of ~1 mV compared with other conditions. This result may be attributed to the optimal Y content in the film, leading to a lower crystal defect. Conversely, the sample treated at the 120 W exhibits the highest hysteresis voltage (10 mV), suggesting that the film can possess a higher density of crystal defects. Fig. 4(b) depicts the variation of V_{Ref} as a function of time for the YbY_xO_y EIS devices prepared under three plasma powers, measured in the pH 7 solutions for 12 h. The change in the reference voltage can be written as $\Delta V_{Ref} = V_{Ref}(t) - V_{Ref}(0)$. The degradation slope of the V_{Ref} variation reflects the stability of an EIS device. The drift phenomenon of an

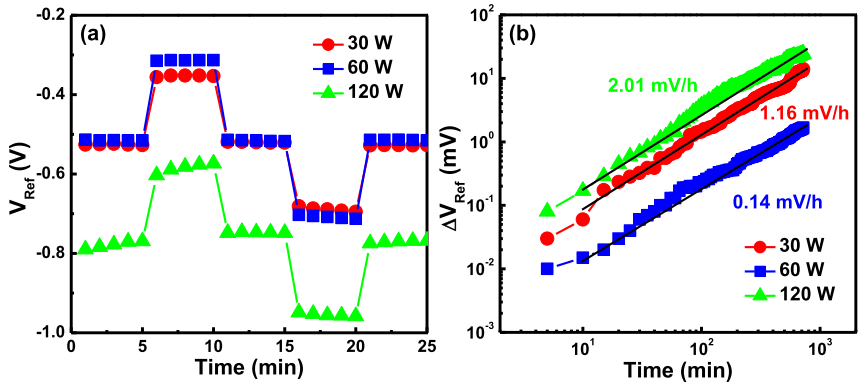

Fig. 4. (a) Hysteresis phenomenon of the YbY_xO_y EIS sensors fabricated at different plasma power conditions in pH loop 7 → 4 → 7 → 10 → 7. (b) Drift characteristics of the YbY_xO_y EIS sensors fabricated at different plasma power conditions in the pH 7 solution.

Please cite this article in press as: T.-M. Pan, et al., Label-free detection of rheumatoid factor using YbY_xO_y electrolyte–insulator–semiconductor devices, Analytica Chimica Acta (2015), http://dx.doi.org/10.1016/j.aca.2015.08.014

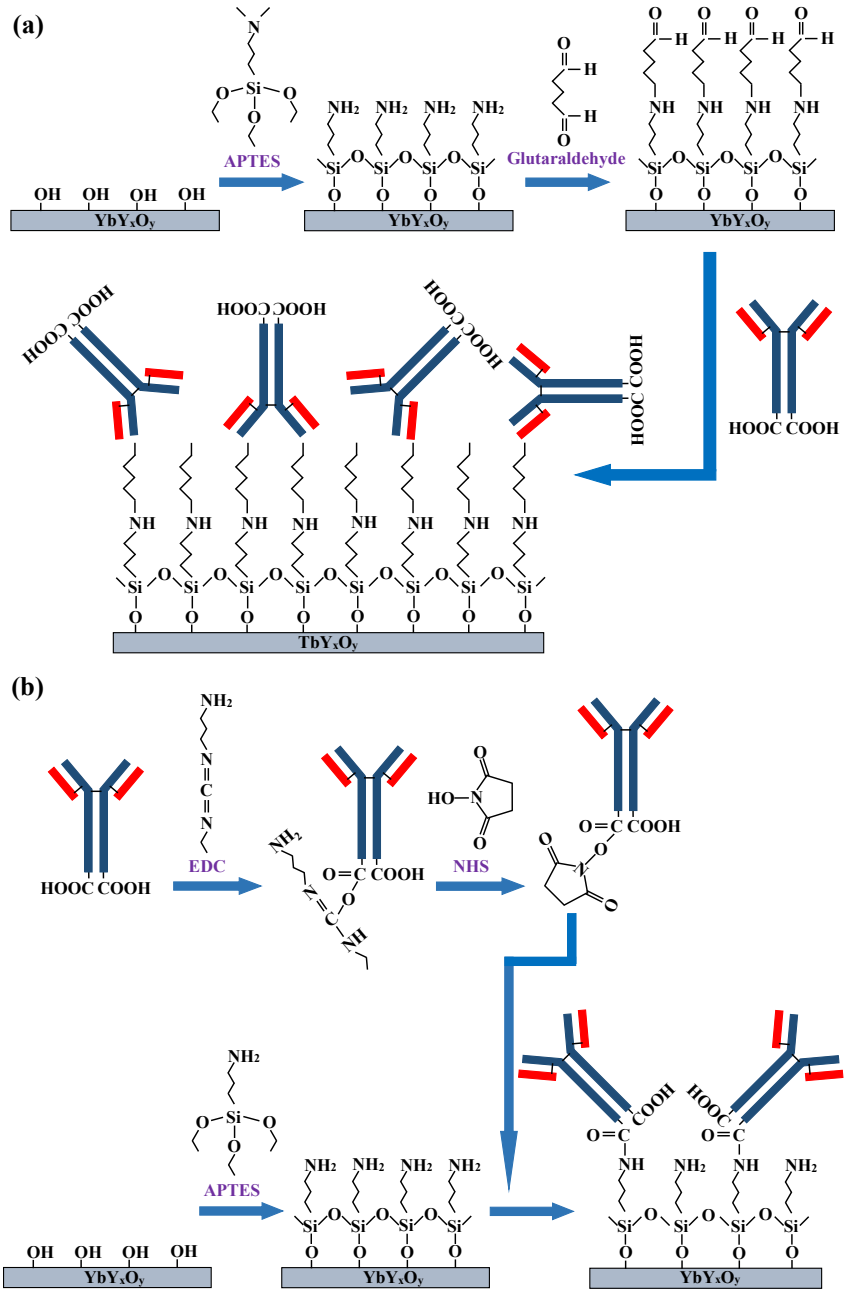

Fig. 5. Scheme of the two elementary activation reactions. (a) The YbY_xO_y surface was modified using APTES solution, the amine groups of APTES were then reacted with GA to produce aldehyde groups. The RF antibody was directly immobilized on the aldehyde groups-modified YbY_xO_y surface. (b) At the first step, the interaction between carboxyl group at the tail of RF antibody and carbodiimide group of EDC results in the functionalization of RF antibody. Subsequently, NHS combined with the functionalized carboxyl group of RF antibody forms the active NHS ester in the RF antibody. Finally, RF antibodies containing active NHS esters were reacted with amine groups of APTES to immobilize onto the YbY_xO_y surface.

ISFET or EIS sensor is that the charged electrolyte ions can penetrate the hydrated layer of a sensing membrane during bias stress, thus leading to a decrease in the effective gate oxide thickness [9]. Therefore, the change in gate capacitance induces non-ideal effects during ISFET (or EIS) pH sensing. The YbY_xO_y EIS sensor prepared at the 60 W condition exhibits a better stability of 0.14 mV/h than other conditions (1.16 mV/h for 30 W and 2.01 mV/h for 120 W). The decrease in a drift rate is due to the lower level of crystal defects, hence causing a lower ionic mobility. On the contrary, a higher drift rate of the sample treated at the 120 W was attributed to the higher density of crystal defects, which result in the higher mobility of ions.

3.3. Detection of various RF concentrations using YbY_xO_y EIS biosensors

Due to the strong and specific binding affinity between antigen and antibody under normal physiological conditions, the receptor-modified EIS can serve as an extremely sensitive sensor with high selectivity. An antibody-modified EIS sensor can be used to detect the corresponding antigen. According to Eq. (1), when the positively charged analytes bind the receptor-modified ISFET device, the increase of surface potential causes a decrease in the V_{Ref} of an ISFET device. In contrast, an increase in the V_{Ref} would arise from

Please cite this article in press as: T.-M. Pan, et al., Label-free detection of rheumatoid factor using YbY_xO_y electrolyte–insulator–semiconductor devices, Analytica Chimica Acta (2015), http://dx.doi.org/10.1016/j.aca.2015.08.014

the reduction of surface potential in the ISFET when negatively charged molecules, such as antigen, DNA, or RNA, bind the p-type EIS. An EIS device as one type of FETs is sensitive to the charge variation at the insulator–electrolyte interface. In principle, the attachment of charged biomolecules to the YbY_xO_y surface should alter its surface potential, leading to the shift in V_{Ref} direction. The modification of YbY_xO_y surface with APTES produces positively charged amino groups ($-NH_2^+$) and M–OH groups on the EIS surface, as shown in Fig. 5(a). These groups operate as receptors of hydrogen ions, which undergo protonation and deprotonation reactions. As shown in Fig. 6(a), it is obvious that the absorption of negatively charged ions onto the APTES-modified EIS sensor causes V_{Ref} position to shift towards the left-hand side. An oxide surface can become charged by reacting with H^+ or OH^- ions due to surface amphoteric reactions depending on the zero point of charge of the oxide. Above the zero point of charge, they lose protons to produce negatively charged surfaces. In contrast, when aldehyde groups of GA were electrostatically absorbed on the surface of APTES-modified EIS, a shift of V_{Ref} to the right was observed in the *C–V* curves. The amine group of APTES was then reacted with GA to yield a positively charged aldehyde group that could form a Schiff base compound with amino group on antibodies. Specific and high affinity binding of antigens on the antibody-modified surface can be detected as a reference voltage shift (ΔV_{Ref}) value, which is determined on the basis of the characteristics of the antibody-modified EIS (or ISFET). Fig. 6(a) shows the *C–V* curves of the YbY_xO_y EIS sensors with APTES–GA modification for different RF antigen concentrations. It was found that the shift in the *C–V* curves shows nonlinearity for different RF antigen concentrations. The inset in Fig. 6(a) demonstrates the V_{Ref} value of the APTES–GA-modified EIS sensors for different serum RF antigen concentrations. This immobilization method showed no proportional change in the V_{Ref} after an EIS sensor was immersed in a solution of serum RF, which suggests that this method will not detect the specific interactions in antigen–antibody. For this instability there are two causes; one is that RF antibodies (e.g. F_{ab} fragment, antigen-binding region) are covalently attached onto an YbY_xO_y surface containing aldehyde groups due to the random orientation of the antibodies on its surface [Fig. 5(a)], thereby leading to lower antigen-binding capacities and efficiencies [23]. During the reaction the GA with the amine-modified YbY_xO_y surface is functionalized with aldehyde groups, which can easily react with the amine groups (F_{ab} fragment) of RF antibody. The other is that the modification of APTES–GA on an EIS surface could not help to select specific antibodies in serum, because GA would bind serum antibodies and other proteins remaining in serum.

The immobilization of the antibody-modified surface for FET detection is very important. The orientation of antibody can be determined by its interaction with antigen. The NH_2-terminus of antibodies binding onto the EIS surface could cause improper orientation of antibodies on its surface to reduce the antigen binding abilities. This drawback can be overcome by using heterobifunctional cross-linker agents and fragment crystallizable-binding proteins [24]. To achieve the high affinity and good stability of antibody-modified EIS surface, we used the EDC and NHS to functionalize RF antibodies, and then immobilized the functionalization of RF antibody on the APTES-modified YbY_xO_y surface. A mixture of EDC and NHS solution was employed to functionalize the carboxyl groups at the tail (F_c fragment) of RF antibody. During this procedure, functionally active NHS esters were obtained due to the reaction of terminal carboxyl groups of RF antibodies. After activation of the NHS, RF antibody containing active NHS esters was then immobilized on YbY_xO_y EIS device. The activated carboxyl functional groups of the RF antibody was coupled covalently by amine functional groups on the YbY_xO_y surface, as shown in Fig. 5(b). In addition, antibodies with uniform and controlled orientation possessed higher activity than those of random orientation [35]. Since the alternating V_{Ref} shifts suggested that the RF antibodies were successfully immobilized onto EIS sensor [Fig. 6(b)], therefore we attempted to convert the affinity of antibody–antigen interactions into a useful analytical signal using EIS as a transducer. Fig. 6(b) shows that the V_{Ref} of the YbY_xO_y EIS device is shifted after serum RF antigen bonds to surface immobilized RF antibody, and this decrease in V_{Ref} is caused by the binding of the negatively charged RF antigen to EIS sensor. The shift in *C–V* curves toward left increases with increasing the serum RF concentration. This behavior is attributed to the RF antigen with a negative charge. The V_{Ref} value linearly decreases with the logarithm of serum RF antigen concentration in the range of

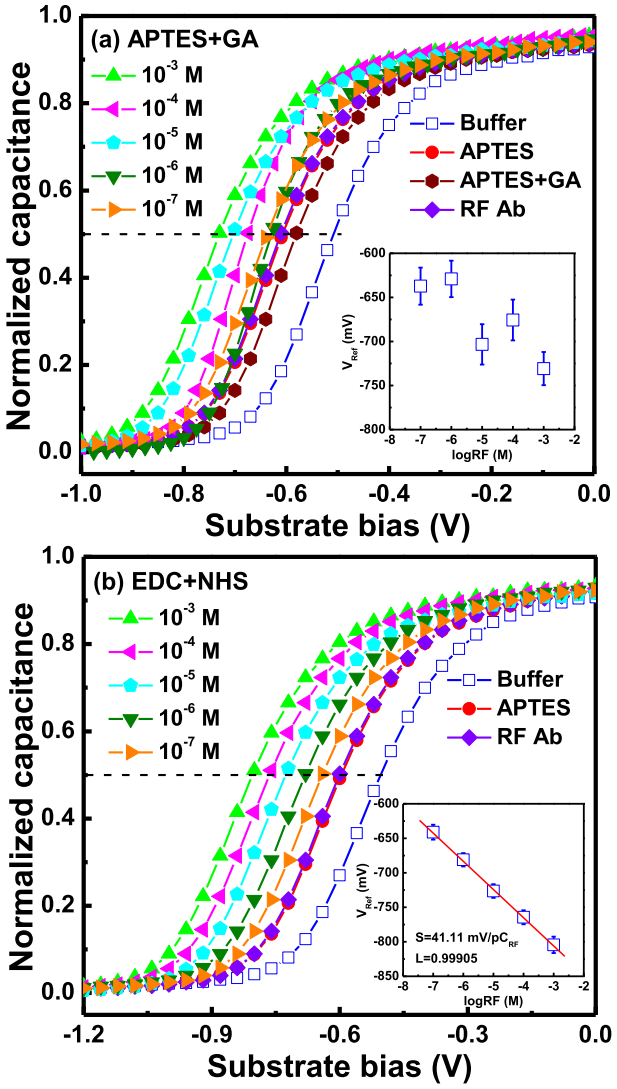

Fig. 6. *C–V* curves of the YbY_xO_y EIS sensors (60 W condition) treated with (a) RF antibodies immobilized on the APTES–GA modified EIS sensor and (b) EDC–NHS functionalize RF antibodies immobilized on the APTES-modified EIS sensor for different serum RF antigen concentrations. Buffer: EIS device without modification, APTES: EIS device with APTES modification, APTES + GA: EIS device with APTES and GA modification, and RF Ab: EIS device with RF antibody immobilization measured buffer solution pH 7. The insets in (a) and (b) show the calibration curves of YbY_xO_y EIS biosensor treated with (a) RF antibodies immobilized on the APTES–GA modified EIS sensor and (b) EDC–NHS functionalize RF antibodies immobilized on the APTES-modified EIS sensor, respectively, for detection of serum RF antigen. Error bars were calculated from the mean values, n = 3.

Please cite this article in press as: T.-M. Pan, et al., Label-free detection of rheumatoid factor using YbY_xO_y electrolyte–insulator–semiconductor devices, Analytica Chimica Acta (2015), http://dx.doi.org/10.1016/j.aca.2015.08.014

10^{-7}–10^{-3} M, as shown in inset of Fig. 6(b). This result may be attributed to the formation of an amide bond between the NH_2-terminus of APTES and the COOH-terminus of antibody due to the cross-linker EDC-NHS molecule leaving the activated surface, resulting in spatial orientation of RF antibodies on the EIS surface to enhance the antibody binding to its antigen. As a result, a higher concentration of RF antigen leads to a larger ΔV_{Ref} value of an EIS sensor. Based on the calibration curve, the sensitivity and linearity of EIS sensor for serum RF are found to be 41.11 mV/pC_{RF} and 99.905%, respectively, within the serum RF concentration range of 10^{-7}–10^{-3} M. As a result, the proposed sensor can detect the serum RF in the abnormal concentration range, e.g. above 2.59×10^{-6} M (40 IU/ml). In comparison with LAT and ELISA, our sensor provides a rapid and label-free diagnostic platform to detect the serum RF. Therefore, this YbY_xO_y EIS biosensor is a very promising candidate to screen RA disease in the earliest stages, monitor medication therapy, and predict the recurrence rate after treatment in the future.

4. Conclusions

We have developed a highly pH sensitive EIS sensor with a thin layer of YbY_xO_y and applied this novel device for pH and serum RF sensing. Based on AES and AFM data, the optimal yttrium content in this oxide with a smooth surface can be formed under the 60 W plasma power. The YbY_xO_y EIS prepared at the 60 W condition exhibits a good linearity ($R^2 = 0.99$) in the pH range 2–12 and possesses an average sensitivity of 65.77 mV/pH exceeding the Nernst limit. Moreover, this condition also has a small hysteresis voltage of ~1 mV and a low drift rate of 0.14 mV/h. Furthermore, we compared two immobilization methods for RF EIS biosensors. The immobilization of antibody functionalized with the EDC and NHS on EIS sensor exhibits a higher sensitivity (41.11 mV/pC_{RF}) for detection of serum RF antigens in the range 10^{-7} to 10^{-3} M, compared to traditional antibody immobilization method via APTES and GA linkage. Due to its easy and inexpensive fabrication, the YbY_xO_y EIS device has a great potential in the application of disposable biosensor.

Acknowledgments

This work was supported by the National Science Council, Taiwan, under contract no. NSC-102-2221-E-182-072-MY3.

References

[1] D.M. Lee, M.E. Weinblatt, Rheumatoid arthritis, Lancet 358 (2001) 903–911.
[2] D. Male, I.M. Roitt, F.C. Hay, Analysis of immune complexes in synovial effusions of patients with rheumatoid arthritis, Clin. Exp. Immunol. 39 (1980) 297–306.
[3] K. Nishimura, D. Sugiyama, Y. Kogata, G. Tsuji, T. Nakazawa, S. Kawano, K. Saigo, A. Morinobu, M. Koshiba, K.M. Kuntz, I. Kamae, S. Kumagai, Meta-analysis: diagnostic accuracy of anti-cyclic citrullinated peptide antibody and rheumatoid factor for rheumatoid arthritis, Ann. Intern. Med. 146 (2007) 797–808.
[4] J.L. Schmitz, J.D. Folds, Evaluation of the rheuma-lex latex agglutination test for detection of rheumatoid factor, J. Clin. Lab. Immunol. 40 (1993) 187–193.
[5] N. Banchuin, K. Janyapoon, S. Sarntivijai, L. Parivisutt, Re-evaluation of ELISA and latex agglutination test for rheumatoid factor detection in the diagnosis of rheumatoid arthritis, Asian Pac. J. Allergy Immunol. 10 (1992) 47–54.
[6] K.A. Drouvalakis, S. Bangsaruntip, W. Hueber, L.G. Kozar, P.J. Utz, H. Dai, Peptide-coated nanotube-based biosensor for the detection of disease-specific autoantibodies in human serum, Biosens. Bioelectron. 23 (2008) 1413–1421.
[7] P. Bergveld, Thirty years of ISFETOLOGY, what happened in the past 30 years and what may happen in the next 30 years, Sens. Actuat. B 88 (2003) 1–20.
[8] T. Matsuo, M. Esashi, H. Abe, pH ISFET's using Al_2O_3, Si_3N_4, and SiO_2 gate thin films, IEEE Trans. Electron Devices 26 (1979) 1856–1857.
[9] L. Bousse, S. Mostarshed, B. van der Schoot, N.F. de Rooij, Comparison of the hysteresis of Ta_2O_5 and Si_3N_4 pH-sensing insulators, Sens. Actuat. B 17 (1994) 157–164.
[10] L. Bousse, H.H. van der Vlekkert, N.F. de Rooij, Hysteresis in Al_2O_3-gate ISFETs, Sen. Actuat. B 2 (1990) 103–110.
[11] J.C. Chou, L.P. Liao, Study of TiO_2 thin films for ion sensitive field effect transistor application with RF sputtering deposition, Jpn. J. Appl. Phys. Part 1 43 (2004) 61–65.
[12] T.M. Pan, K.M. Liao, Influence of oxygen content on the structural and sensing characteristics of Y_2O_3 sensing membrane for pH-ISFET, Sen. Actuat. B 128 (2007) 245–251.
[13] V. Jankovic, J.P. Chang, HfO_2 and ZrO_2–based microchemical ion sensitive field effect transistor (ISFET) sensors: simulation & experiment, J. Electrochem. Soc. 158 (2011) P115–P117.
[14] J. Paivasaari, M. Putkonen, L. Niinisto, A comparative study on lanthanide oxide thin films grown by atomic layer deposition, Thin Solid Films 472 (2005) 275–281.
[15] M. Fanciulli, G. Scarel, Rare Earth Oxide Thin Film: Growth, Characterization, and Applications, Springer, Berlin, 2007.
[16] O. Engstrom, B. Raeissi, S. Hall, O. Buiu, M.C. Lemme, H.D.B. Gottlob, P.K. Hurley, K. Cherkaoui, Navigation aids in the search for future high-k dielectrics: physical and electrical trends, Solid State Electron 51 (2007) 622–626.
[17] T.M. Pan, W.S. Huang, Physical and electrical characteristics of a high-k Yb_2O_3 gate dielectric, Appl. Surf. Sci. 255 (2009) 4979–4982.
[18] T.M. Pan, W.S. Huang, Effects of oxygen content on the structural and electrical properties of thin Yb_2O_3 gate dielectrics, J. Electrochem. Soc. 156 (2009) G6–G11.
[19] Y. Zhao, M. Toyama, K. Kita, K. Kyuno, A. Toriumi, Moisture-absorption-induced permittivity deterioration and surface roughness enhancement of lanthanum oxide films on silicon, Appl. Phys. Lett. 88 (2006) 072904.
[20] T. Schroeder, G. Lupina, J. Dabrowski, A. Mane, Ch. Wenger, G. Lippert, H.J. Mussig, Titanium-added praseodymium silicate high-k layers on Si(001), Appl. Phys. Lett. 87 (2005) 022902.
[21] Y. Zhao, K. Kita, K. Kyuno, A. Toriumi, Higher-k $LaYO_x$ films with strong moisture resistance, Appl. Phys. Lett. 89 (2006) 252905.
[22] R.A. Williams, H.W. Blanch, Covalent immobilization of protein monolayers for biosensor applications, Biosens. Bioelectron. 9 (1994) 159–167.
[23] B. Lu, M.R. Smyth, R. Okennedy, Oriented immobilization of antibodies and its applications in immunoassays and immunosensors, Analyst 121 (1996) 29R–32R.
[24] S.K. Vashist, E. Lam, S. Hrapovic, K.B. Male, J.H.T. Luong, Immobilization of antibodies and enzymes on 3-aminopropyltriethoxysilane-functionalized bioanalytical platforms for biosensors and diagnostics, Chem. Rev. 114 (2014) 11083–11130.
[25] V. Crivianu-Gaita, M. Thompson, Immobilization of Fab' fragments onto substrate surfaces: A survey of methods and applications, Biosens. Bioelectron. 70 (2015) 167–180.
[26] C.K. Dixit, S.K. Vashist, B.D. MacCraith, R. O'Kennedy, Multisubstrate-compatible ELISA procedures for rapid and high-sensitivity immunoassays, Nat. Protoc. 6 (2011) 439–445.
[27] D.E. Yates, S. Levine, T.W. Healy, Site-binding model of the electrical double layer at the oxide/water interface, J. Chem. Soc. Faraday Trans. 170 (1974) 1807–1818.
[28] L. Bousse, N.F. de Rooij, P. Bergveld, Operation of chemically sensitive field-effect sensors as a function of the insulator-electrolyte interface, IEEE Trans. Electron Devices 30 (1983) 1263–1270.
[29] R.E.G. van Hal, J.C.T. Eijkel, P. Bergveld, A novel description of ISFET sensitivity with the buffer capacity and double-layer capacitance as key parameter, Sen. Actuat. B 24 (1995) 201–205.
[30] T.M. Pan, C.H. Cheng, C.D. Lee, Yb_2O_3 thin films as a sensing membrane for pH-ISFET application, J. Electrochem. Soc. 156 (2009) J108–J111.
[31] G.M. da Silva, S.G. Lemos, L.A. Pocrifka, P.D. Marreto, A.V. Rosario, E.C. Pereira, Development of low-cost metal oxide pH electrodes based on the polymeric precursor method, Anal. Chim. Acta 616 (2008) 36–41.
[32] Y. Miao, J. Guan, J. Chen, Ion sensitive field effect transducer-based biosensors, Biotechnol. Adv. 21 (2003) 527–534.
[33] C.W. Liao, J.C. Chou, T.P. Sun, S.K. Hsiung, J.H. Hsieh, Preliminary investigations on a glucose biosensor based on the potentiometric principle, Sen. Actuat. B 123 (2007) 720–726.
[34] J.C. Chou, Y.F. Wang, Preparation and study on the drift and hysteresis properties of the tin oxide gate ISFET by the sol-gel method, Sens. Actuat. B 86 (2002) 58–62.
[35] M. Soellner, K. Dickson, B. Nilsson, R. Raines, Site-specific protein immobilization by Staudinger ligation, J. Am. Chem. Soc. 125 (2003) 11790–11791.

Please cite this article in press as: T.-M. Pan, et al., Label-free detection of rheumatoid factor using YbY_xO_y electrolyte–insulator–semiconductor devices, Analytica Chimica Acta (2015), http://dx.doi.org/10.1016/j.aca.2015.08.014